Learning Null Geodesics for Gravitational Lensing Rendering in General Relativity

Appendix

Mingyuan Sun[1] Zheng Fang[1,†] Jiaxu Wang[2] Kunyi Zhang[3] Qiang Zhang[2,4] Renjing Xu[2,†]
[1]Northeastern University [2]The Hong Kong University of Science and Technology (Guangzhou)
[3]Sichuan University [4]Beijing Innovation Center of Humanoid Robotics Co., Ltd.

A1. Additional Experiments

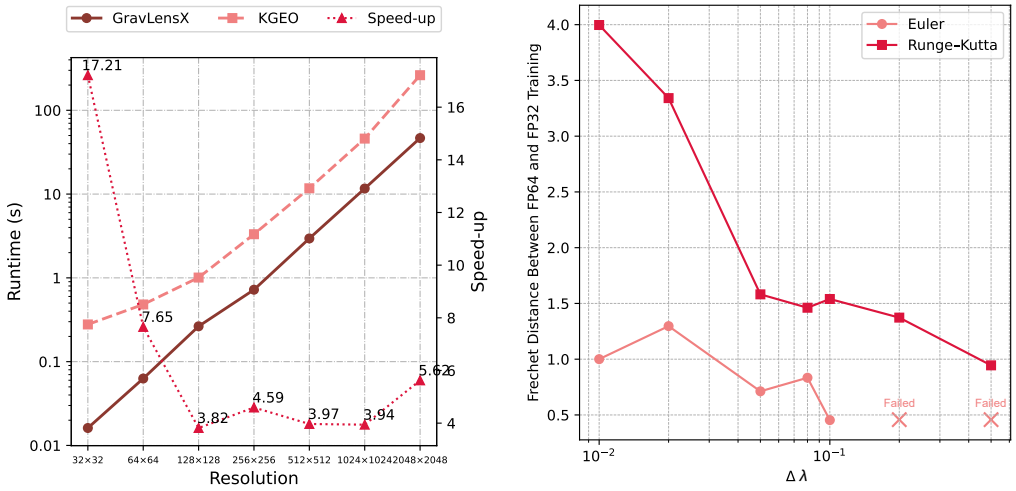

Figure A1. **(Left)** Runtime comparison between kgeo and GravLensX. 100 points are sampled for each ray. **(Right)** Frechet distances between paths using FP32 and FP64.

kgeo is an implementation of Gralla and Lupsasca [4]'s work that provides a fast and accurate solution to the null geodesic equations in Kerr spacetime with elliptic integrals. For single-black-hole scenario, we benchmarked kgeo on a Xeon Gold 5218 CPU by launching 16 parallel processes to fully utilize all cores, and compared this to `GravLensX` on a single NVIDIA RTX 3090 GPU. `GravLensX` yields speed-ups of roughly 3.8× to 17.2× (see Figure A1 Left). More importantly, for the multi-black-hole scenarios we consider in our paper leveraging the superposed Kerr metric, Gralla and Lupsasca [4]'s theory cannot be utilized.

A2. Implementation Details

We set $N_{\text{coarse}} = N_{\text{fine}} = 10$. R^{bh} is set as 20. Detailed parameters for generating data are listed in Tab. A1. Taichi [5] and PyTorch [1] are used to render the black hole systems and train the neural networks.

†Corresponding authors.

Table A1. Parameters of generating geodesic data.

System	P^{bh}	M^{bh}	A^{bh}	l^{in}	l^{out}	in-black-hole radius
2 Black Holes	(-30, 0, 0), (30, 0, 0)	1, 1	1, 1	1.6	100	1.8
3 Black Holes	$(30, 10\sqrt{3}, 0), (-30, 10\sqrt{3}, 0), (0, -20\sqrt{3}, 0)$	1, 1, 1	1, 1, -1	2.2	100	2.25

As for the training process, we use MLPs with 12 hidden layers and residual connections, employing SoftPlus as the activation function. For the near field network, each layer contains 200 neurons. For the far field network, each layer has 128 neurons in the 2-black-hole system and 200 neurons in the 3-black-hole system. The learning rate is set as 0.001 with default Adam optimizer. We trained the far-field network on 4 RTX 3090 GPUs and the near-field network on single RTX 3090. The time for generating data and training the model on RTX 3090 is around 13.8 GPU hours for every near-field NN and 33.5 GPU hours for the far-field NN. For the 3-black-hole scenario, this is equivalent to rendering a 63 minutes video in 30 FPS with Euler method. For more complex systems, the training time grows linearly with the number of black holes. We did not investigate much on the training acceleration, and we believe the training time can be largely reduced by using more advanced optimizers, model structures, etc.

A3. Superposed Black Hole Metric

Black hole metric, e.g. Schwarzschild metric [9], is the solution to Einstein field equations under certain assumptions. We primarily utilize the Kerr metric [7] that describes a rotating black hole to characterize the black hole system, as adopted by earlier studies [2, 6, 8]. Kerr metric in Cartesian coordinates is defined as

$$\mathrm{d}s^2 = -\mathrm{d}t^2 + \mathrm{d}x^2 + \mathrm{d}y^2 + \mathrm{d}z^2 + \frac{2mr^3}{r^4 + a^2z^2}\left(\mathrm{d}t + \frac{r(x\,\mathrm{d}x + y\,\mathrm{d}y)}{a^2 + r^2} + \frac{a(y\,\mathrm{d}x - x\,\mathrm{d}y)}{a^2 + r^2} + \frac{z}{r}\,\mathrm{d}z\right)^2, \tag{A1}$$

where the Boyer-Lindquist radius r is implicitly given by

$$x^2 + y^2 + z^2 = r^2 + a^2\left(1 - \frac{z^2}{r^2}\right). \tag{A2}$$

m and a are the mass and the angular momentum of the black hole, respectively. t, x, y, and z are the coordinates in the spacetime. ds represents an infinitesimal spacetime interval, which captures the separation between two nearby events in spacetime. With Equation (A1), The metric tensor for these four coordinates can be calculated as

$$g_{ab} = \eta_{ab} + \frac{2mr^3}{r^4 + a^2z^2}\ell_a\ell_b, \tag{A3}$$

with

$$\ell = \left[1, \frac{rx + ay}{r^2 + a^2}, \frac{ry - ax}{r^2 + a^2}, \frac{z}{r}\right]^{\mathsf{T}}, \tag{A4}$$

where η_{ab} is the Minkowski metric tensor. We use an affine parameter λ to parameterize the geodesic as done by d'Ascoli et al. [3] and Porter et al. [8]. Let $p = [t, x, y, z]^{\mathsf{T}}$ denote the spacetime coordinates. The geodesic equation can be written as

$$\frac{\mathrm{d}^2p^\mu}{\mathrm{d}\lambda^2} + \Gamma^\mu_{\alpha\beta}\frac{\mathrm{d}p^\alpha}{\mathrm{d}\lambda}\frac{\mathrm{d}p^\beta}{\mathrm{d}\lambda} = 0 \tag{A5}$$

in which λ is the affine parameter, ensuring the path is parameterized in a way that preserves the affine properties of the curve. $\Gamma^\mu_{\alpha\beta}$ is the Christoffel symbol describing how coordinates change in curved spacetime, which can be calculated from the metric tensor as

$$\Gamma^\mu_{\alpha\beta} = \frac{1}{2}g^{\mu\nu}\left(\frac{\partial g_{\nu\alpha}}{\partial p^\beta} + \frac{\partial g_{\nu\beta}}{\partial p^\alpha} - \frac{\partial g_{\alpha\beta}}{\partial p^\nu}\right), \tag{A6}$$

where $g^{\mu\nu}$ is the inverse of the metric tensor, satisfying

$$g^{\mu\nu}g_{\nu\alpha} = \delta^\mu_\alpha = \begin{cases} 1 & \text{if } \mu = \alpha \\ 0 & \text{if } \mu \neq \alpha \end{cases} \tag{A7}$$

Calculating the partial derivative term in the Christoffel symbol is the most computationally expensive part in solving the geodesic equation. In order to calculate the second order derivative of each coordinate w.r.t. λ in Equation (A5), we need to obtain the derivative of the time coordinate w.r.t. λ, $\frac{\mathrm{d}t}{\mathrm{d}\lambda}$. According to the general relativity, light travels along null geodesics, indicating that the derivatives of the four coordinates p satisfy

$$g_{\mu\nu}\frac{\mathrm{d}p^{\mu}}{\mathrm{d}\lambda}\frac{\mathrm{d}p^{\nu}}{\mathrm{d}\lambda}=0. \tag{A8}$$

Solving this equation yields $\frac{\mathrm{d}t}{\mathrm{d}\lambda}$. By discretizing the λ and iterately solve the spacetime coordinate at each lambda step.

A4. Proof for $l^{\text{straight}} \leq l^{\text{geodesic}}$ and Its Convergence

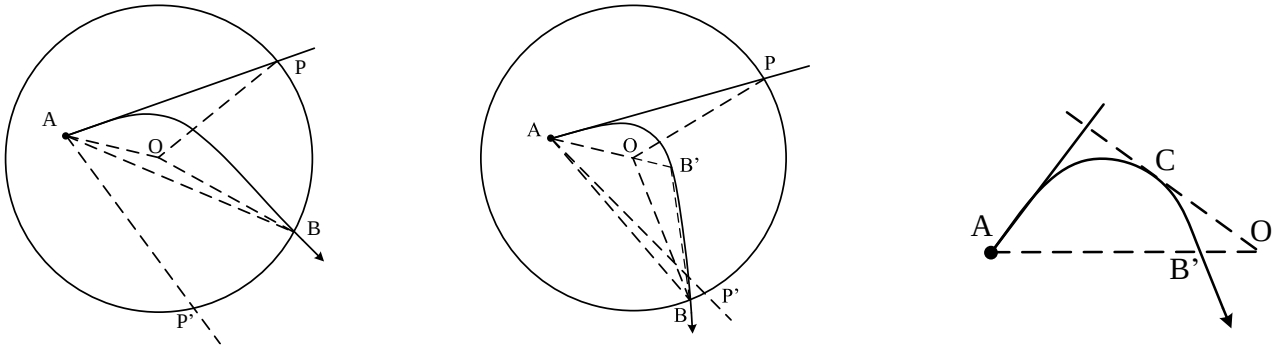

Figure A2. Different cases of intersections.

Suppose a ray is casted from point A to point B in the near-field region with radius R centered at O, where B is its first crossing point to the boundary. The nonzero acceleration $\mathrm{d}^2r/\mathrm{d}\lambda^2 < 0$ caused by gravity bends the ray towards the center. d is the initial direction of the ray and P is the point where the straight line from position P with direction d intersects the boundary.

Proposition A4.1. *Let L_{AB} be the length of the ray from point A to point B. The following inequality holds:*

$$L_{AB} \geq |AP|. \tag{A9}$$

Proof. Consider the plane expanded by points A, O, and B. Let P' be the reflection of P across line AO.

Case 1: Point B is on the arc $\widehat{PP'}$ As shown in Figure A2a, through cosine law, we have

$$\begin{aligned}|AP| &= R^2 + |AO|^2 - 2R|AO|\cos(\angle AOP),\\ |AB| &= R^2 + |AO|^2 - 2R|AO|\cos(\angle AOB).\end{aligned}$$

Clearly, $\angle AOB \geq \angle AOP$, which implies $L_{AB} \geq |AB| \geq |AP|$, where the latter equality only holds when B is on P or P'.

Case 2: Point B is not on the arc $\widehat{PP'}$ As shown in Figure A2b, extending line AO intersects the trajectory AB firstly at point B'. Assume the crossing point B' lies on AO (see Figure A2c). Draw line OC through point O such that OC is tangent to curve AB', with C being the point of tangency. Denote the position and speed of the curve at point C as $p_c = (x_c, y_c)^\mathsf{T}$, $v_c = (-k \cdot x_c, -k \cdot y_c)^\mathsf{T}$ in which k is a constant value, as its direction is parallel to the tangent line across the coordinates origin. Also, the acceleration is parallel to the direction v_c, thus the trajectory of the ray after C should be a straight line pointing towards O. This contradicts our assumption that the curve would continue bending until it reaches AO at B', leading to the conclusion that B' cannot lie on AO and should instead intersect the extension of line AO towards the O end. Now we have

$$L_{AB} = L_{AB'} + L_{B'B} \geq |AO| + |OB'| + |B'B| \geq |AO| + |OB| \geq |AP|.$$

□

In our method, we iteratively step over the ray path to conduct ray tracing. We denote the start point and direction as A_0 and d_0. At each step, we calculate the length of A_0P_0, where P_0 is the point of intersection between the boundary and the straight line cast from A_0 in the direction of d_0. Then we step with length $s_0 = |A_0P_0|$ on the ray path and obtain next point A_1 and direction d_1. This iteration process is conducted until the point is sufficiently near to the boundary, i.e., sufficiently close to B.

Proposition A4.2. *Given a point on a ray path influenced by the gravity in the near-field, we have*

$$\lim_{T\to\infty}\sum_{t=0}^{T} s_t = L_{A_0B}. \tag{A10}$$

Proof. Through our definition, we have

$$s_t \geq 0, \qquad \forall t \in \mathbb{N}.$$

By Proposition A4.1, it holds that

$$\sum_{t=0}^{T} s_t \leq L_{A_0B} < +\infty, \qquad \forall T \in \mathbb{N},$$

indicating that $\sum_{t=0}^{T} s_t$ converges, and

$$\lim_{t\to\infty} s_t = 0.$$

Assume $r := L_{A_0B} - \sum_{t=0}^{\infty} s_t > 0$, pick B' on the path so that $L_{B'B} = r$. Clearly A_t converges to B' as t increases, and it holds that

$$\lim_{t\to\infty} s_t = s_{B'},$$

in which $s_{B'}$ is the distance from B' to the boundary across its tangent line. As B' does not overlap with B,

$$\lim_{t\to\infty} s_t = s_{B'} > 0,$$

this contradicts to the aforementioned condition, therefore $r > 0$ does not hold, implying that

$$\sum_{t=0}^{\infty} s_t = L_{A_0B}.$$

□

References

[1] Jason Ansel, Edward Yang, Horace He, Natalia Gimelshein, Animesh Jain, Michael Voznesensky, Bin Bao, Peter Bell, David Berard, Evgeni Burovski, Geeta Chauhan, Anjali Chourdia, Will Constable, Alban Desmaison, Zachary DeVito, Elias Ellison, Will Feng, Jiong Gong, Michael Gschwind, Brian Hirsh, Sherlock Huang, Kshiteej Kalambarkar, Laurent Kirsch, Michael Lazos, Mario Lezcano, Yanbo Liang, Jason Liang, Yinghai Lu, CK Luk, Bert Maher, Yunjie Pan, Christian Puhrsch, Matthias Reso, Mark Saroufim, Marcos Yukio Siraichi, Helen Suk, Michael Suo, Phil Tillet, Eikan Wang, Xiaodong Wang, William Wen, Shunting Zhang, Xu Zhao, Keren Zhou, Richard Zou, Ajit Mathews, Gregory Chanan, Peng Wu, and Soumith Chintala. PyTorch 2: Faster Machine Learning Through Dynamic Python Bytecode Transformation and Graph Compilation. In *29th ACM International Conference on Architectural Support for Programming Languages and Operating Systems, Volume 2 (ASPLOS '24)*. ACM, 2024. 1

[2] Andy Bohn, William Throwe, François Hébert, Katherine Henriksson, Darius Bunandar, Mark A Scheel, and Nicholas W Taylor. What does a binary black hole merger look like? *Classical and Quantum Gravity*, 32(6):065002, 2015. 2

[3] Stéphane d'Ascoli, Scott C Noble, Dennis B Bowen, Manuela Campanelli, Julian H Krolik, and Vassilios Mewes. Electromagnetic emission from supermassive binary black holes approaching merger. *The Astrophysical Journal*, 865(2):140, 2018. 2

[4] Samuel E Gralla and Alexandru Lupsasca. Null geodesics of the kerr exterior. *Physical Review D*, 101(4):044032, 2020. 1

[5] Yuanming Hu, Tzu-Mao Li, Luke Anderson, Jonathan Ragan-Kelley, and Frédo Durand. Taichi: a language for high-performance computation on spatially sparse data structures. *ACM Transactions on Graphics (TOG)*, 38(6):201, 2019. 1

[6] Oliver James, Eugénie von Tunzelmann, Paul Franklin, and Kip S Thorne. Gravitational lensing by spinning black holes in astrophysics, and in the movie interstellar. *Classical and Quantum Gravity*, 32(6):065001, 2015. 2

[7] Roy P. Kerr. Gravitational field of a spinning mass as an example of algebraically special metrics. *Phys. Rev. Lett.*, 11:237–238, 1963. 2

[8] Kaitlyn Porter, Scott C Noble, Eduardo M Gutierrez, Joaquin Pelle, Manuela Campanelli, Jeremy Schnittman, and Bernard J Kelly. A parameter study of the electromagnetic signatures of an analytical mini-disk model for supermassive binary black hole systems. *arXiv preprint arXiv:2407.04089*, 2024. 2

[9] Karl Schwarzschild. Über das gravitationsfeld eines massenpunktes nach der einsteinschen theorie. *Sitzungsberichte der königlich preussischen Akademie der Wissenschaften*, pages 189–196, 1916. 2